Flow-induced properties of nanotube-filled polymer materials

SEMEN B. KHARCHENKO[1]*, JACK F. DOUGLAS[1]*, JAN OBRZUT[1], ERIC A. GRULKE[2] AND KALMAN B. MIGLER[1]*

[1]Polymers Division, National Institute of Standards and Technology, Gaithersburg, Maryland 20899-8544, USA
[2]University of Kentucky, Department of Chemical and Materials Engineering, Lexington, Kentucky 40506-0503, USA
*e-mail: semen.kharchenko@nist.gov; jack.douglas@nist.gov; kalman.migler@nist.gov

Published online: 25 July 2004; doi:10.1038/nmat1183

Carbon nanotubes (CNTs) are under intense investigation in materials science owing to their potential for modifying the electrical conductivity σ, shear viscosity η, and other transport properties of polymeric materials. These particles are hybrids of filler and nanoscale additives because their lengths are macroscopic whereas their cross-sectional dimensions are closer to molecular scales. The combination of extended shape, rigidity and deformability allows CNTs to be mechanically dispersed in polymer matrices in the form of disordered 'jammed' network structures. Our measurements on representative network-forming multiwall nanotube (MWNT) dispersions in polypropylene indicate that these materials exhibit extraordinary flow-induced property changes. Specifically, σ and η both decrease strongly with increasing shear rate, and these nanocomposites exhibit impressively large and negative normal stress differences, a rarely reported phenomenon in soft condensed matter. We illustrate the practical implications of these nonlinear transport properties by showing that MWNTs eliminate die swell in our nanocomposites, an effect crucial for their processing.

Onsager[1] first explained the tendency of highly anisotropic rod-like and plate-like particles (for example, tobacco mosaic virus and clay particles in solution) to form orientationally ordered nematic phases, and his pioneering work has since been refined into a rich and technologically significant theory of liquid-crystalline material properties and phase transitions[2]. The applicability of this theory to ensembles of extended objects is questionable, however, when they become so large that brownian motion is insignificant and the attainment of equilibrium thus impossible. This condition arises, for example, when highly extended particles are placed in a viscous matrix, precisely the nature of carbon nanotube and exfoliated clay[3] polymer 'nanocomposites'. Such materials are inherently out of equilibrium, and can be expected to exhibit properties distinct from their equilibrium liquid-crystalline counterparts.

The strong interest in carbon nanotubes (CNTs) dispersed into polymeric materials stems from their ability to affect thermal[4], electrical[5] and rheological[6] properties at relatively small concentrations. CNT additives have found manufacturing applications in electrostatic painting, protective coatings for electronic components[7] and flammability reduction[8]. Use of CNTs, however, requires an understanding of how processing conditions (mixing, moulding, extrusion) influence nanocomposite properties.

Despite the high elastic modulus of carbon nanotubes, their small cross-sectional dimensions and extreme length relative to this dimension allow them to bend[9] substantially in response to inter-tube interactions under processing conditions. At concentrations greater than random close-packing for rigid tubular objects, this bending leads to the formation of a disordered web-like structure of substantial mechanical integrity[10]. These non-equilibrium systems have been referred to as 'jammed solids'[11] or 'dispersion gels'[10], and are encountered in a wide range of everyday materials (for example, colloidal suspensions, pastes and granular media)[12]. The presence of a nanotube network interpenetrating the polymer matrix creates additional and large contributions to nanocomposite viscoelasticity. What kind of transport properties can be expected from this peculiar state of matter, beyond an increase in stiffness and electrical and thermal conductivity?

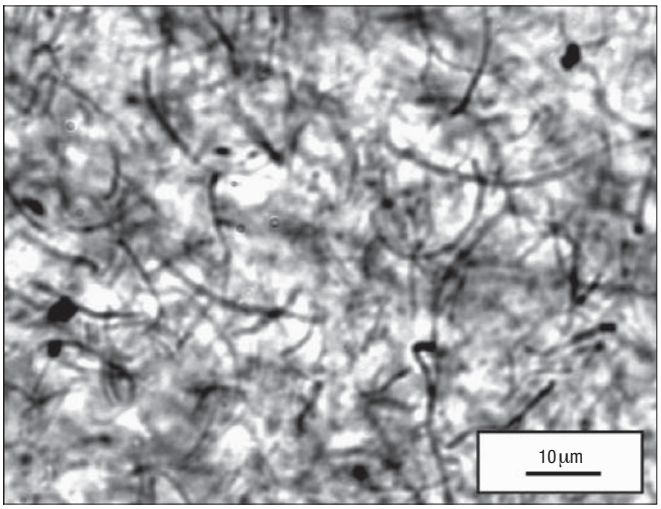

Figure 1 Morphology of MWNT/PP nanocomposites. This optical microscopy image of $\phi = 0.01$ nanocomposite, obtained using a ×100 objective, demonstrates good dispersion of the MWNTs and reveals a polydispersity in nanotube length and shape. The uniformity of dispersion remains at higher concentrations, but it becomes more difficult to resolve the individual tubes.

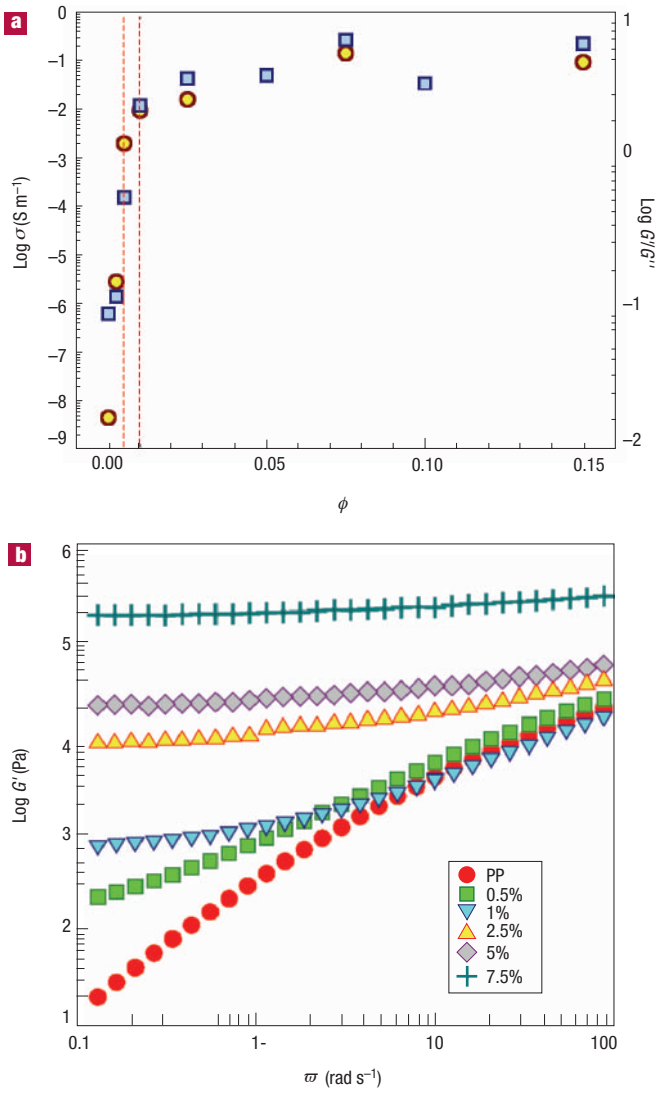

Figure 2 Characterization of the transport property transitions in MWNT/PP nanocomposites. a, The insulator–conductor transition (left *y* axis) is shown by the circles and the liquid-like to solid-like transition (right *y* axis) by the squares ($T = 200$ °C). The (G'/G'') ratio is measured at $\omega = 0.1$ rad s^{-1}. The red dashed lines indicate the percolation threshold range. **b**, The increase in the elasticity (G') of nanocomposites with nanotube content.

First, we briefly consider the geometrical configuration of the MWNTs in a polypropylene (PP) matrix. Imaging this structure at high volume fractions is difficult due to the strong optical adsorption by CNTs, but we can obtain representative optical images for intermediate MWNT concentrations, as shown in Fig. 1. The MWNT volume fraction ϕ in this figure is 0.01, which is close to the geometrical percolation concentration where the CNT network first forms, and where the conductivity and stiffness of the nanocomposite increase by orders of magnitude, as described below.

Next, we characterize the large changes in viscoelasticity and conductivity for which polymer composites containing CNT are well known. In Fig. 2, we show simultaneous measurements of the electrical conductivity, σ, and the shear moduli (G', G'') of our nanocomposites. G' can be thought of as a measure of 'stiffness' and G'' provides a measurement of viscous resistance to deformation. The ratio (G'/G''), otherwise known as the inverse of the 'loss tangent' $(G''/G' \equiv \tan\delta)$, is a measure of the composite 'firmness' and we compare this basic quantity to σ. We observe that both (G'/G'') and σ increase with ϕ and that this variation becomes rapid for ϕ in the range from 0.0025 to 0.01. The transport property percolation thresholds for conductivity and firmness are both in the concentration range 0.0025 to 0.01 (indicated by the dashed red lines in Fig. 2a), and this range is comparable to an order of magnitude estimate of the geometrical percolation threshold. For specific comparison, we note that the percolation threshold for overlapping needles in the range between 0.01 and 0.001 corresponds to an aspect-ratio range between 100 and 1,000 (ref. 13). Independent measurement of the aspect ratio of our nanotubes indicates a value near 1,000 before processing, and between 300 and 400 after processing. We also point out that the sharp increase in σ occurs at a somewhat lower level of ϕ than that for (G'/G''), consistent with the expectation that connectivity percolation should precede the percolation of rigidity[14].

We see from Fig. 2 that adding MWNT to the PP matrix increases the conductivity by an impressive seven orders of magnitude as a percolating structure forms. Similar changes have been noted in earlier works[15], showing the attractiveness of using MWNT additives for modifying the electrical conductivity of polymeric materials[5].

These additives also lead to an appreciable change in the nanocomposite elasticity (G'), which increases by a factor of the order of 10^4 (Fig. 2b). We further observe that G' and G'' become independent of frequency as ϕ is varied through the gelation concentration $\phi_c \approx 0.01$ at which the viscoelastic response changes from 'liquid-like' to 'solid-like'. This finding is qualitatively similar to previous observations on aqueous CNT dispersions[16], so we can conclude that the elastic effects arise primarily from the nanotube network. An examination of the concentration dependence of G' and G'' indicates that it scales as $\phi^{2.7\pm0.2}$, which is also consistent with former aqueous CNT-dispersion measurements. Networks of sterically entangled solutions of semiflexible biopolymers, such as F-actin[17], exhibit a similar scaling of G' and G'' with ϕ, suggesting that this

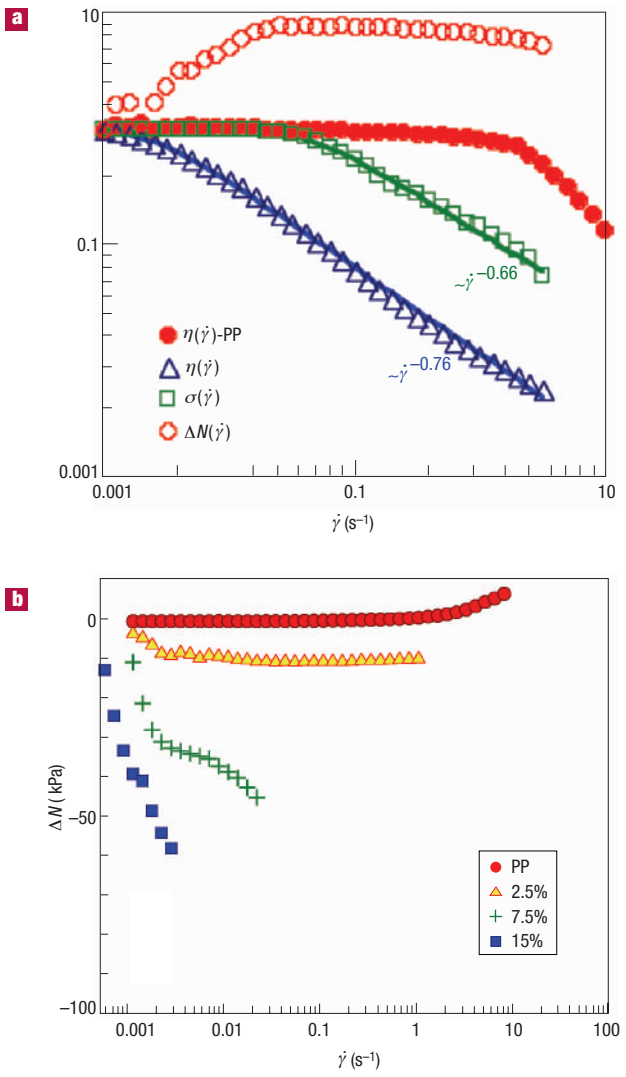

Figure 3 Modification of transport properties during flow. a, The normalized viscosity, normal force and electrical conductivity of the $\phi = 0.025$ nanocomposite ($T = 200$ °C), and solid lines are Carreau fits (see text). The normalized viscosity of the unfilled PP (red circles) is shown to demonstrate the role of the MWNT network at the onset of shear thinning. Properties are normalized by the reference 'low' shear-rate values for $\dot{\gamma} = 0.001$ s^{-1} (note that the viscosity of the 2.5% MWNT/PP nanocomposite is larger by about a factor of 100 than that of the matrix). **b**, Effect of the MWNT content on the normal force measurements.

concentration scaling may hold generally for disordered networks of semiflexible fibres. We next focus on the more novel problem of the nonlinear flow properties of this class of nanocomposites.

First, we characterize the general nature of the fluid flow and the prevalence of thermal relaxation processes in our nanocomposites in terms of dimensionless measures of the flow rate, the Péclet number (ratio of the shear rate to the rate of particle reorientation by brownian motion) and the Reynolds number (ratio of the inertial to viscous dissipation energies). The Péclet number is estimated from the MWNT rotary diffusion coefficient $Pe = \dot{\gamma}/D_r$, where $\dot{\gamma}$ is the shear rate, and where we use the Doi-Edwards estimate[18] $D_r = k_B T \ln(a_r)/(3L^3)(nL^3)^2$ appropriate for semi-dilute fibre suspensions. In this expression, k_B is the Boltzmann constant, L is the nanotube length (measured to be approximately 15 μm), a_r is the nanotube aspect ratio (taken to be approximately 400)[19], and n is the number density of nanotubes, and η is the shear viscosity. The large matrix viscosity and the highly extended nature of the tubes make the Péclet number huge in our nanocomposites[20] ($10^{14} - 10^{16}$), whereas the Reynolds number is vanishingly small ($Re \approx 10^{-11} - 10^{-8}$). We may infer from these parameter values that CNT brownian motion is rather limited.

The above rheological and electrical transport properties are strongly modified by the presence of a steady-state shear field, as shown in Fig. 3a. We examine the case of $\phi = 0.025$, which is representative of the concentration range $\phi > \phi_c$. Notably, $\eta(\dot{\gamma})$ exhibits a much stronger shear thinning over the $\dot{\gamma}$ range indicated, compared to the near constancy of $\eta(\dot{\gamma})$ for the pure PP matrix ($\eta(\dot{\gamma})$-PP; Fig. 3a). This shear thinning of the nanocomposite can be well described by the simple Carreau equation[21], $\eta(\dot{\gamma})/\eta(\dot{\gamma}\rightarrow 0) \approx [1 + (\dot{\gamma}\tau_\eta)^2]^{-0.38} \approx \dot{\gamma}^{-0.76}$, where the characteristic time $\tau_\eta \approx 20$ s defining the reduced shear rate $\dot{\gamma}\tau_\eta$ and the onset of shear thinning is estimated from a fit to the experimental data. The asymptotic shear-thinning exponent –0.76 is notably close to the one observed in highly entangled polymer melts and concentrated polymer solutions[21,22]. The Carreau equation has been used successfully to describe $\eta(\dot{\gamma})$ in many complex fluids, including those near the critical point for phase separation[22].

It is common practice in polymer science to estimate the magnitude of the complex dynamic shear viscosity $\eta^*(\omega)$, obtained by subjecting a material to a low amplitude oscillatory shear by simply replacing $\dot{\gamma}$ in $\eta(\dot{\gamma})$ with ω. We found that this phenomenological Cox–Merz rule[21], which often holds to a good approximation for entangled polymer fluids, did not apply to our percolated MWNT nanocomposites ($\phi > \phi_c$). This finding is consistent with former observations on concentrated aqueous nanotube dispersions[16], and clay nanocomposites[3]. Apparently, some aspects of the rheology of CNT dispersions are similar to that of entangled polymer fluids[22,23], while others are not.

Our simultaneous conductivity measurements on the $\phi = 0.025$ nanocomposite, carried out in the shear-gradient direction, show an analogous dependence on $\dot{\gamma}$ (Fig. 3a). Thus, the capacity of the nanotube network to transmit electric charges decreases with $\dot{\gamma}$ in a similar fashion. The decrease in σ can be concisely described by fitting our data to an expression similar to the Carreau equation, $\sigma(\dot{\gamma})/\sigma(\dot{\gamma}\rightarrow 0) \approx [1 + (\dot{\gamma}\tau_\sigma)^2]^{-0.33} \approx \dot{\gamma}^{-0.66}$, where the characteristic time defining the onset of the decrease in σ is related to τ_η as $\tau_\sigma = 0.24\ \tau_\eta$. These are the first simultaneous measurements of electrical and rheological properties of polymer nanocomposites and we expect this technique to become a useful characterization tool.

The decrease of both transport properties with increasing $\dot{\gamma}$ reflects changes in the network structure, which evidently becomes less effective at transmitting shear stress and electrical current under flow conditions. Clearly, if the nanotubes begin to orient in the flow field, the conductivity should be reduced for two reasons: the number of tube–tube contacts will decrease as the tube orientations become less random, and because $\sigma(\dot{\gamma})$ measurements are made in a direction perpendicular to flow, we are then probing conductivity along the less-conductive direction of the tubes[24]. Previous measurements on carbon-black-filled polyethylene[25] have established that the conductivity of that type of composite is dominated by the contact resistances between the filler particles separated by the polymer matrix. This decrease in conductivity is interpreted to arise primarily from a disruption of local tube contacts induced by shear. The disruption of the 'bonds' of the nanotube network from a 'bound' to a 'free' state has also been predicted to lead to a precipitous drop in the ability of the network to sustain stress on large length scales and thus to a drop in η as in the case of fractal flocs of spheres[26]. Owing to the high aspect ratio of the tubes, these effects are observed at much lower concentrations than in the carbon black. Apparently, σ and η are both sensitive to subtle changes in the local contact geometry of the nanotube network that are difficult to discern morphologically. Although the exact relation between the shear

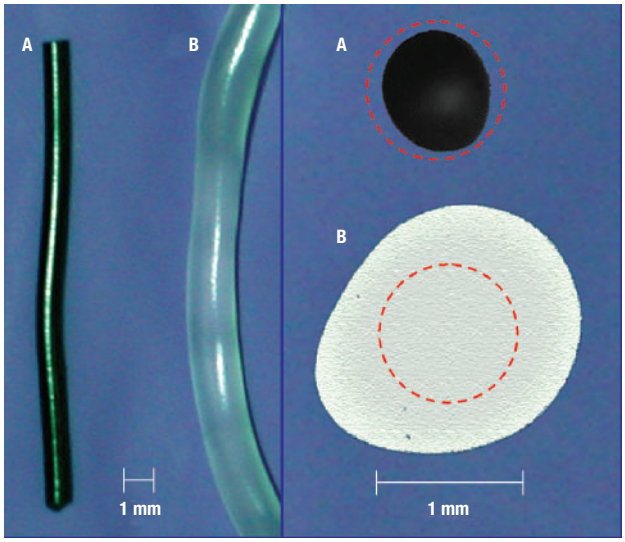

Figure 4 Suppression of die swell by MWNT filler. Extrudate A is the nanocomposite ($\phi = 0.025$; $T = 200$ °C) where die contraction is observed. For comparison, the dashed line in the cross-section indicates the die diameter. B indicates the control measurement for the unfilled PP polymer matrix from which the nanocomposite was made. In the latter case, there is a substantial die swell and shape distortion under these extrusion conditions ($\dot{\gamma} = 1{,}150\ s^{-1}$, $T = 180$ °C).

dependence and the transport properties shown in Fig. 3a remains open, it seems clear that these effects have a similar qualitative origin.

In order to manufacture these polymer composites into usable shapes, we must understand how the network structure acts to influence their processing behaviour. 'Normal forces' provide a measure of the stored elastic energy during flow, and arise from the stretching and alignment of the fluid microstructure along flow streamlines. Two manifestations of these forces are rod-climbing (fluid rising up a rotating stirring bar) and 'die swell' (expansion of a fluid jet of fluid upon exiting a pipe)[21]. Normal stresses are typically measured by sandwiching thin slabs of material between two parallel plates, applying a shear field and measuring the resulting thrust on the plates. This inter-plate force vanishes in newtonian fluids, but is non-zero in complex fluids, such as polymer fluids and colloidal dispersions. Typically, the thrust acts to push the plates away from each other in high molecular mass ('entangled') polymers, corresponding to a positive normal force. In the case of a parallel-plate geometry, the measured normal force is actually a difference of the normal stress differences, $\Delta N \equiv N_1 - N_2$ (the normal stress differences N_1 and N_2 are defined as $(\tau_{11} - \tau_{22})$ and $(\tau_{22} - \tau_{33})$, respectively, where τ_{ii} are the normal stresses acting along the flow (1), flow gradient (2) and vorticity (3) directions. A positive ΔN is observed in our nanocomposite for $\phi \leq \phi_c$, where the polymer matrix dominates the rheological response (Fig. 3b), but ΔN becomes large and negative for $\phi > \phi_c$. Moreover, the magnitude of ΔN increases sharply with ϕ at a fixed $\dot{\gamma}$. Given the peculiar nature of this rheological observation, we measured the normal force in a cone-and-plate geometry (for the $\phi = 0.025$ sample) and were able to determine that $N_1 < 0$. Although we have not quantitatively measured N_2, we can determine that its magnitude is significantly lower than N_1 based on these measurements. Thus, we conclude that the negative sign of the normal force is due to a negative N_1.

The observation of negative normal stresses is a remarkable phenomenon that is rarely reported in soft condensed matter. This phenomenon has sometimes been observed, for example, in lyotropic liquid-crystalline polymers (LCP), where there is a competition between flow-induced orientation and ordering into a thermodynamically driven nematic state[2,27]. Apart from liquid-crystalline polymers, negative normal forces have been reported in 'attractive' emulsions (including mayonnaise)[28], in concentrated suspensions of large ('non-colloidal') spherical particles at high Péclet numbers dispersed in both newtonian[29–31] and viscoelastic fluids[32], and for platelet-shaped clay (kaolin) particles[33]. In addition to these 'pastes', negative normal stresses have been observed in simulations of other jammed materials such as granular systems[34]. Although these studies agree on the occurrence of negative normal forces, the sign of the corresponding normal stress components was found to differ from one system to another. Specifically, N_1 and ΔN were both found to be negative in refs 28, 32 and 33, whereas ΔN was found to be positive (owing to $N_2 < N_1 < 0$) in refs 29 and 31. These observations emphasize that the measurement of ΔN alone is insufficient to determine even the sign of N_1 or N_2, so that the rheological experiments in more than one geometry are required to determine the normal stresses, as described above.

Of direct relevance to the present work, there have been recent reports of negative ΔN in both single-wall[35] and multiwall[36] CNT dispersions in low-viscosity solvents where the effect has been interpreted in terms of liquid-crystalline ordering[35] and correlated with vorticity alignment[36]. Although the observation of a negative ΔN is consistent with our nanocomposite measurements, the magnitude of ΔN that we find is larger than these former measurements by orders of magnitude. Moreover, these normal forces develop instantaneously under shear flow in the nanocomposite, rather than taking an extended period of time (up to an hour) or requiring critical shear rates to become established. These differences are crucial to our observations of die-swell suppression below, because the polymer melt itself exhibits a large positive ΔN, and a negative ΔN of large magnitude is required to compensate this polymer-matrix effect. This interplay between compensating non-newtonian effects is unique to the present system.

Although the origin of the negative normal stresses in CNT dispersions remains unresolved, we can obtain insights into this phenomenon from recent simulations exhibiting it. Brownian-dynamics simulations for suspensions of spheres at high shear rates[37] ($Pe \to \infty$) have indicated large negative normal stresses arising from lubrication forces that couple the motions of nearby particles, leading to formation of transient particle-network structures that notably do not exhibit significant orientational ordering. Measurements on suspensions of spherical particles in both newtonian and non-newtonian polymer fluids have confirmed the existence of negative normal forces under the conditions indicated by the simulations[29–33]. A combination of viscous and dry friction effects contributes to sustaining network junctions in real suspensions under flow, as established from both simulations and experiments on fibre dispersions under flow[38]. We can also anticipate that the deformability of the suspended particles themselves should influence ΔN. Indeed, simulation has recently indicated that fibre flexibility alone can give rise to a negative ΔN in highly dilute fibre dispersions[39] because of competing tendencies of the flow streamlines to fold and align the filaments. On the basis of these simulations, former measurements and our own observations, we postulate that both the large-scale deformation of the nanotube network and nanotube deformation on a local scale contribute to the large negative ΔN that we find. In particular, we expect the mesh scale of the nanotube network to stretch along the shear-flow direction, while compressing along the shear-gradient direction. These distorted tube elements would then exert a negative ΔN.

The existence of large negative normal stresses can be expected to have a dramatic impact on processing these complex materials, as well as their ultimate material properties. Because the extrusion of the nanocomposite is a basic processing operation for which normal stresses are known to be important, we focus on this particular flow. The extrusion of high-molecular-mass polymer such as the PP matrix of

our nanocomposite normally exhibits significant die swell. One might expect, based on existing models[21], a negative normal stress to lead to a contraction or little change in the dimensions of an extruded jet of nanocomposite, similar to earlier reports on extrusion of suspensions of non-colloidal (Pe→∞) spheres and liquid-crystalline melts[32,40]. To test this intriguing possibility in the MWNT composites, we extruded a $\phi = 0.025$ sample for which both ΔN and N_1 were found to be negative in the range of $\dot{\gamma}$ investigated. Figure 4 shows that the cross-section of the extrudate indeed becomes smaller than the die area (by a factor of 0.77), while the extrusion of the pure PP matrix material under the same nominal conditions yields a substantial die swell of the extrudate (corresponding to a swelling of up to six times the die area). In addition, the pure PP suffers from a shape-distortion instability causing the extrudate cross-section to become non-circular, whereas this effect is greatly diminished in the nanocomposite. Such distortion is a common processing difficulty in the manufacture of plastic materials by extrusion.

In summary, the micrometre-scale of carbon nanotube length makes these particles non-brownian when suspended in polymeric matrices, whereas their nanometric cross-section facilitates their deformation under flow, despite their nominal rigidity. These hybrid dimensional and physical characteristics facilitate the formation of disordered solid materials in which the particles bend to form a self-sustaining structure interpenetrating the polymer matrix. The large property contrast and the stabilization against phase separation arising from network formation make these 'blends' attractive for many technological applications. Our measurements show that the viscosity and electrical conductivity can be substantially modified by flow, creating the potential for fabricating 'smart' materials (for example, pressure-sensitive switches) that could actuate based on these property changes. The suppression of die swell of extruded polymers by adding a relatively small amount of MWNTs ($\phi \approx 0.01$) also offers a powerful tool for controlling dimensional characteristics and surface distortion in manufacturing commodity composites. Our observations of strongly nonlinear rheology under flow (shear thinning and large negative normal stresses) imply that these fluids should exhibit other 'anomalous' flow characteristics (for example, droplet distortion and thread break-up) that are quite unlike newtonian fluids, and which are crucial for their processing and for controlling the properties of this promising class of materials.

METHODS

The MWNTs were grown in a chemical vapour deposition reactor by the catalytic decomposition of hydrocarbons[8], and MWNT/PP blends were formed by melt blending with volume fractions (ϕ) ranging from 0.0025 to 0.15. As shown previously[8], the distribution of MWNT in PP (by an ultrasound-assisted dispersion, followed by the use of the twin-screw melt mixer) leads to a relatively uniformly dispersed material without the necessity of using surfactants or surface functionalization of the tubes.
Rheology measurements were conducted in the temperature range 180 °C to 220 °C under N_2, using 25 mm diameter parallel plates (ARES) as well as a Paar Physica Universal Dynamic Spectrometer USD 200 rheometer set at a gap of about 0.8 mm; additionally, a 25 mm diameter cone-and-plate fixture (ARES) with the cone angle of 0.0434 rad set a gap of 0.0559 mm was used. The oscillatory frequency experiments were run at strain magnitudes in the range 2–0.08%. These conditions were selected so that the modulus depending on polymer frequency would be independent of the strain magnitude.

GENERAL INFORMATION

Certain equipment, instruments or materials are identified in this paper in order to adequately specify the experimental details. Such identification does not imply recommendation by the National Institute of Standards and Technology nor does it imply the materials are necessarily the best available for the purpose.

Received 11 February 2004; accepted 18 June 2004; published 25 July 2004.

References

1. Onsager, L. The effect of shape on the interaction of colloidal particles. *Ann. NY Acad. Sci.* **51,** 627–659 (1949).
2. Larson, R. G. Arrested tumbling in shearing flows of liquid-crystal polymers. *Macromolecules* **23,** 3983–3992 (1990).
3. Ren, J. X. & Krishnamoorti, R. Nonlinear viscoelastic properties of layered-silicate-based intercalated nanocomposites. *Macromolecules* **36,** 4443–4451 (2003).
4. Huxtable, S. T. *et al.* Interfacial heat flow in carbon nanotube suspensions. *Nature Mater.* **2,** 731–734 (2003).
5. Baughman, R. H., Zakhidov, A. A. & de Heer, W. A. Carbon nanotubes - the route toward applications. *Science* **297,** 787–792 (2002).
6. Potschke, P., Fornes, T. D. & Paul, D. R. Rheological behavior of multiwalled carbon nanotube/polycarbonate composites. *Polymer* **43,** 3247–3255 (2002).
7. Terrones, M. Science and technology of the twenty-first century: Synthesis, properties and applications of carbon nanotubes. *Ann. Rev. Mater. Res.* **33,** 419–501 (2003).
8. Kashiwagi, T. *et al.* Thermal degradation and flammability properties of poly(propylene)/carbon nanotube composites. *Macromol. Rapid Commun.* **23,** 761–765 (2002).
9. Yakobson, B. I., Brabec, C. J. & Bernholc, J. Nanomechanics of carbon tubes: Instabilities beyond linear response. *Phys. Rev. Lett.* **76,** 2511–2514 (1996).
10. Bicerano, J., Douglas, J. F. & Brune, D. A. Model for the viscosity of particle dispersions. *J. Macromol. Sci. Rev. Macromol. Chem. Phys.* **C39,** 561–642 (1999).
11. Liu, A. J. & Nagel, S. R. Nonlinear dynamics: Jamming is not just cool any more. *Nature* **396,** 21–22 (1998).
12. Cloitre, M., Borrega, R., Monti, F. & Leibler, L. Glassy dynamics and flow properties of soft colloidal pastes. *Phys. Rev. Lett.* **90,** 068303 (2003).
13. Garboczi, E. J., Snyder, K. A., Douglas, J. F. & Thorpe, M. F. Geometrical percolation-threshold of overlapping ellipsoids. *Phys. Rev. E* **52,** 819–828 (1995).
14. Head, D. A., Levine, A. J. & MacKintosh, F. C. Distinct regimes of elastic response and deformation modes of cross-linked cytoskeletal and semiflexible polymer networks. *Phys. Rev. E* **68,** 061907 (2003).
15. Bin, Y. Z., Kitanaka, M., Zhu, D. & Matsuo, M. Development of highly oriented polyethylene filled with aligned carbon nanotubes by gelation/crystallization from solutions. *Macromolecules* **36,** 6213–6219 (2003).
16. Kinloch, I. A., Roberts, S. A. & Windle, A. H. A rheological study of concentrated aqueous nanotube dispersions. *Polymer* **43,** 7483–7491 (2002).
17. MacKintosh, F. C., Kas, J. & Janmey, P. A. Elasticity of semiflexible biopolymer networks. *Phys. Rev. Lett.* **75,** 4425–4428 (1995).
18. Doi, M. & Edwards, S. F. *The Theory of Polymer Dynamics* (Oxford Univ. Press, New York 1986).
19. Safadi, B., Andrews, R. & Grulke, E. A. Multiwalled carbon nanotube polymer composites: Synthesis and characterization of thin films. *J. Appl. Polym. Sci.* **84,** 2660–2669 (2002).
20. Powell, R. L. Rheology of suspensions of rodlike particles. *J. Stat. Phys.* **62,** 1073–1094 (1991).
21. Tanner, R. I. *Engineering Rheology* (Oxford Univ. Press, New York 2000).
22. Douglas, J. F. "Shift" in polymer blend phase-separation temperature in shear flow. *Macromolecules* **25,** 1468–1474 (1992).
23. Shaffer, M. S. P. & Windle, A. H. Analogies between polymer solutions and carbon nanotube dispersions. *Macromolecules* **32,** 6864–6866 (1999).
24. Du, F. M., Fischer, J. E. & Winey, K. I. Coagulation method for preparing single-walled carbon nanotube/poly(methyl methacrylate) composites and their modulus, electrical conductivity, and thermal stability. *J. Polym. Sci. Polym. Phys.* **41,** 3333–3338 (2003).
25. Martin, J. E. & Heaney, M. B. Reversible thermal fusing model of carbon black current-limiting thermistors. *Phys. Rev. B* **62,** 9390–9397 (2000).
26. Bossis, G., Meunier, A. & Brady, J. F. Hydrodynamic stress on fractal aggregates of spheres. *J. Chem. Phys.* **94,** 5064–5070 (1991).
27. Baek, S. G., Magda, J. J. & Larson, R. G. Rheological differences among liquid-crystalline polymers. 1. the 1st and 2nd normal stress differences of Pbg solutions. *J. Rheol.* **37,** 1201–1224 (1993).
28. Montesi, A., Peña, A. A. & Pasquali, M. Vorticity alignment and negative normal stresses in sheared attractive emulsions. *Phys. Rev. Lett.* **92,** 058303 (2004).
29. Zarraga, I. E., Hill, D. A. & Leighton, D. T. The characterization of the total stress of concentrated suspensions of noncolloidal spheres in Newtonian fluids. *J. Rheol.* **44,** 185–220 (2000).
30. Kolli, V. G., Pollauf, E. J. & Gadala-Maria, F. Transient normal stress response in a concentrated suspension of spherical particles. *J. Rheol.* **46,** 321–334 (2002).
31. Singh, A. & Nott,P . R. Experimental measurements of the normal stresses in sheared Stokesian suspensions. *J. Fluid Mech.* **490,** 293–320 (2003).
32. Aral, B. K. & Kalyon, D. M. Viscoelastic material functions of noncolloidal suspensions with spherical particles. *J. Rheol.* **41,** 599–620 (1997).
33. Moan, M., Aubry, T. & Bossard, F. Nonlinear behavior of very concentrated suspensions of plate-like kaolin particles in shear flow. *J. Rheol.* **47,** 1493–1504 (2003).
34. Brady, J. F. & Carpen, I. C. Second normal stress jump instability in non-Newtonian fluids. *J. Non-Newton. Fluid Mech.***102,** 219–232 (2002).
35. Davis, V. A. *et al.* Phase behavior and rheology of SWNTs in superacids. *Macromolecules* **37,** 154–160 (2004).
36. Lin-Gibson, S., Pathak, J. A., Grulke, E. A., Wang, H. & Hobbie, E. K. Elastic-flow instability in nanotube suspensions. *Phys. Rev. Lett.* **92,** 048302 (2004).
37. Sierou, A. & Brady, J. F. Rheology and microstructure in concentrated noncolloidal suspensions. *J. Rheol.* **46,** 1031–1056 (2002).
38. Schmid, C. F. & Klingenberg, D. J. Mechanical flocculation in flowing fiber suspensions. *Phys. Rev. Lett.* **84,** 290–293 (2004).
39. Becker, L. E. & Shelley, M. J. Instability of elastic filaments in shear flow yields first-normal-stress differences. *Phys. Rev. Lett.* **87,** 198301 (2001).
40. Jerman, R. E. & Baird, D. G. Rheological properties of copolyester liquid-crystalline melts. 1. Capillary rheometry. *J. Rheol.* **25,** 275–292 (1981).

Correspondence and requests for materials should be addressed to S.B.K., J.F.D. and K.B.M.

Competing financial interests

The authors declare that they have no competing financial interests.